Author Manuscript

Author Manuscript

Author Manuscript

Author Manuscript

HHS Public Access

Author manuscript

Cancer Res. Author manuscript; available in PMC 2018 October 01.

Published in final edited form as:

Cancer Res. 2017 October 01; 77(19): 5395–5408. doi:10.1158/0008-5472.CAN-17-1571.

Mitotic vulnerability in triple-negative breast cancer associated with LIN9 is targetable with BET inhibitors

Jennifer M. Sahni[1,9], **Sylvia S. Gayle**[1,9], **Bryan M. Webb**[1], **Kristen L. Weber-Bonk**[1], **Darcie D. Seachrist**[1], **Salendra Singh**[2], **Steven T. Sizemore**[3], **Nicole A. Restrepo**[4], **Gurkan Bebek**[5], **Peter C. Scacheri**[2,6], **Vinay Varadan**[2], **Matthew K. Summers**[7], and **Ruth A. Keri**[1,2,6,8,*]

[1]Department of Pharmacology, Case Western Reserve University, Cleveland, OH 44106

[2]Case Comprehensive Cancer Center, Case Western Reserve University, Cleveland, OH 44106

[3]Department of Radiation Oncology, The Ohio State University, Columbus, OH 43210

[4]Department of Epidemiology and Biostatistics, Case Western Reserve University, Cleveland, OH 44106

[5]Center for Proteomics and Bioinformatics, Case Western Reserve University, Cleveland, OH 44106

[6]Department of Genetics and Genome Sciences, Case Western Reserve University, Cleveland, OH 44106

[7]Department of Cancer Biology, Lerner Research Institute, Cleveland Clinic, Cleveland, OH 44195; current address: Department of Radiation Oncology, The Ohio State University, Columbus, OH 43210

[8]Department General Medical Sciences-Oncology, Case Western Reserve University, Cleveland, OH 44106

Abstract

Triple-negative breast cancers (TNBC) are highly aggressive, lack FDA-approved targeted therapies, and frequently recur, making the discovery of novel therapeutic targets for this disease imperative. Our previous analysis of the molecular mechanisms of action of Bromodomain and extraterminal protein inhibitors (BETi) in TNBC revealed these drugs cause multinucleation, indicating BET proteins are essential for efficient mitosis and cytokinesis. Here, using live cell imaging, we show that BET inhibition prolonged mitotic progression and induced mitotic cell death, both of which are indicative of mitotic catastrophe. Mechanistically, the mitosis regulator *LIN9* was a direct target of BET proteins that mediated the effects of BET proteins on mitosis in TNBC. While BETi have been proposed to function by dismantling super-enhancers (SE), the *LIN9* gene lacks a SE but was amplified or overexpressed in the majority of TNBCs. In addition, its mRNA expression predicted poor outcome across breast cancer subtypes. Together, these

[*]**Corresponding author**: Ruth A. Keri, 2109 Adelbert Road, Cleveland, Ohio 44106-4965, Phone: (216) 368-3495, Fax: (216) 368-1300, keri@case.edu.

[9]These authors contributed equally to this work.

Conflict of interest: The authors declare no potential conflicts of interest.

Author Manuscript Author Manuscript Author Manuscript Author Manuscript

results provide a mechanism for cancer selectivity of BETi that extends beyond modulation of SE-associated genes and suggest that cancers dependent upon LIN9 overexpression may be particularly vulnerable to BETi.

Keywords

LIN9; mitotic catastrophe; breast cancer; BET inhibitors; gene regulation and transcriptional control

INTRODUCTION

Proper progression through mitosis is critical for maintaining cell function and viability. To prevent mitotic defects and subsequent chromosomal instability, the expression and activity of mitotic proteins are carefully controlled by several mechanisms, including ubiquitin-mediated protein degradation, phosphorylation, miRNA regulation, and transcription. FOXM1, E2F family members, the MuvB core complex (composed of LIN9, LIN52, LIN37, LIN54, and RBBP4), B-MYB, and NF-Y are master transcriptional regulators of mitosis and are responsible for the timely expression of genes encoding crucial mitosis proteins, including *AURKA*, *AURKB*, *PLK1*, and *CCNB1* (1). When these transcription factors are dysregulated, abnormal mitosis occurs which can produce cells with aberrant nuclei (potentially with damaged DNA) and induce cell death pathways, senescence, and/or oncogenesis (1). One mechanism that avoids genomic instability is mitotic catastrophe, a process that occurs due to chromosomal abnormalities or abnormal mitosis, coincides with mitotic arrest, and leads to one of three cell fates: irreversible senescence, death during mitosis, or death immediately following mitotic exit (2, 3). Prior to the execution of these oncosuppressive mechanisms, a characteristic early-stage indicator of mitotic catastrophe is the appearance of multiple nuclei and/or micronuclei (3, 4). Either early entry into mitosis or failed mitosis can trigger mitotic catastrophe (2, 3). In cancer, mitotic catastrophe can be induced in response to treatment with ionizing radiation and anti-cancer agents including microtubule-targeting and DNA-damaging drugs, and the inhibition of mitotic catastrophe provides a mechanism for tumor initiation and the development of chemoresistance (5–7).

Triple-negative breast cancer (TNBC) is the most aggressive subtype of breast cancer, and there is a paucity of effective targeted therapies for this disease. These tumors are treated with traditional chemotherapy such as taxanes and anthracyclines, and while they initially respond, they frequently recur within three years (8). It is therefore critical we develop new treatment strategies for this devastating disease. We and others have recently reported that bromodomain and extraterminal protein inhibitors (BETi) are efficacious in multiple models of TNBC (9–13). We further discovered that BETi induce the formation of large, multinucleated cells followed by apoptosis and senescence, suggesting these drugs cause mitotic catastrophe (12). BETi selectively target the BET family of epigenetic readers by binding to the bromodomain pockets of BET proteins (BRD2, BRD3, BRD4, and BRDT). This prevents recruitment of these proteins to chromatin, thus suppressing their transcriptional activity (14). BETi are efficacious in mouse models of diverse cancers (15) and are currently being investigated in early phase clinical trials. The selectivity for cancers

Author Manuscript Author Manuscript Author Manuscript Author Manuscript

and broad therapeutic windows observed with BETi in mice have been suggested to result from the selective disruption of super-enhancers (SE), exceptionally large clusters of enhancers that control expression of cell identity genes and, in cancer, critical oncogenes (16, 17). BRD4 disproportionately accumulates at SEs compared to typical enhancers. Hence, dismantling SEs at oncogenes would have a greater transcriptional effect and be more impactful in cancer cells that depend on those genes rather than normal cells. This model provides a mechanism to preferentially silence oncogenes which could in turn inhibit tumor formation, growth, and progression, while sustaining viability of normal tissues. However, it remains unclear whether the primary mechanism for selectivity of BETi in cancers involves disruption of SEs at oncogenes, or if cancer cells may be particularly sensitive to the suppression of viability genes that extend beyond oncogenes and those involved in maintaining cell identity. Identifying the processes underlying cellular responses to these inhibitors will be essential for improving patient selection for future clinical trials, predicting therapeutic response and resistance, and rationally discovering optimal added therapies for evoking synergistic tumor responses.

Here, we show for the first time that suppression of BET protein activity leads to a significant delay or death in mitosis in TNBC cells. Together with the generation of multinucleated cells, these findings indicate BETi induce mitotic catastrophe. This process is initiated by the direct suppression of *LIN9* as well as other cell cycle regulatory transcription factors, including *FOXM1* and *MYBL2*. None of these genes contain SEs, disputing the concept that tumor response to BETi solely relies on the dismantling of such enhancers. Notably, *LIN9* is amplified or overexpressed in the majority of TNBC tumors and its suppression mimics BETi. This indicates that LIN9 may be an exploitable therapeutic target in TNBC that can be selectively silenced with BETi.

MATERIALS AND METHODS

Cell culture and reagents

MDA-MB-231, MDA-MB-468, HCC1143, HCC70, and HCC38 cells from American Type Culture Collection (ATCC) were grown in RPMI-1640 supplemented with 10% FBS and maintained at 37°C with 5% CO_2. MDA-MB-231 cells were authenticated in 2013 by STR profiling (BDC Molecular Biology Core Facility, University of Colorado). All other cell lines were purchased from ATCC between 2008 and 2010. Upon receipt, they were thawed and expanded for freezing ~75, 1 mL vials. From each of these vials, ~75, 1 mL vials were generated. All experiments were then performed with cells that were within 10 passages of these secondary vials. MDA-MB-231 and HCC1143 cells were tested in 2013 for *Mycoplasma pulmonis* and *Mycoplasma spp*. by IDEXX RADIL (Columbia, MO). JQ1 was dissolved in dimethyl sulfoxide (DMSO). Transient mRNA silencing was performed using the following siRNAs (Dharmacon): Non-targeting siRNA #2 (D-001810-02-20), siFOXM1 (L-009762-00), siE2F2 (L-003260-00), siE2F8 (L-014407-01), siLIN9 (L-018918-01), and siMYBL2 (L-010444-00).

Author Manuscript Author Manuscript Author Manuscript Author Manuscript

Caspase 3/7 cleavage stain

Cells were treated with vehicle or JQ1 for 72 hours. Media and cells were then harvested and stained with CellEvent Caspase-3/7 Green Reagent (Molecular Probes, R37111) for two hours according to the provided protocol. GFP-positive (apoptotic) and GFP-negative (live) cells were counted using a Countess II FL (Thermo Fisher, AMQAF1000) with an EVOS GFP light cube (Thermo Fisher, AMEP4651).

Senescence-associated β-galactosidase activity stain

Staining was performed as previously described (12).

Live cell imaging

HCC38 and MDA-MB-231 cells were treated with vehicle or 1000 nM JQ1 and imaged using the IncuCyte Zoom System (Essen BioScience) for four days. Images were collected at 20× every 20 minutes. Individual cells were tracked from mitotic entry to mitotic exit and the time course of events determined. Relative cell proliferation was analyzed using the IncuCyte software Confluence application.

RNA analysis

RNA analysis was performed as previously described (12) using the following TaqMan Gene Expression Assays (Thermo Fisher): *CCNB1* (Hs01030099_m1); *E2F2* (Hs00231667_m1); *E2F8* (Hs00226635_m1); *FOXM1* (Hs01073586_m1); *KIF2C* (Hs00901710_m1); *KIF20A* (Hs00993573_m1); *LIN9* (Hs00542748_m1); *LIN37* (Hs00375230_m1); *MYBL2* (Hs00942543_m1); *PLK1* (Hs00983227_m1); *GAPDH* (Hs02758991_g1).

In vivo studies

All *in vivo* experiments were performed with approval from the Institutional Animal Care and Use Committee at Case Western Reserve University, which is certified by the American Association of Accreditation for Laboratory Animal Care. Mouse xenograft studies were previously reported with tissues being used for the current analysis (12). Briefly, MDA-MB-231 or MDA-MB-468 cells were xenografted into the two inguinal mammary fat pads of adult female NOD/scid/γ (NSG) mice. Once palpable tumors formed, mice were randomized into two treatment groups: vehicle (1:1 propylene glycol:water) or JQ1 (50 mg/kg IP daily). After 28 (MDA-MB-231) or 32 (MDA-MB-468) days of treatment, tumors were removed and processed for RT-qPCR analysis.

Nuclear morphology

FOXM1, *E2F2*, *E2F8*, *LIN9*, or *MYBL2* were transiently silenced in MDA-MB-231 cells grown on sterile glass coverslips. After five days, cells were fixed with 3.7% formaldehyde/1xPBS, permeabilized with 0.1% Triton X-100/1xPBS, and blocked with 1% BSA/1xPBS. Texas Red-X phalloidin (Invitrogen, T7471) was used to label F-actin. Nuclei were counterstained with Vectashield hard set mounting medium with DAPI (Vector Labs, H-1500).

Author Manuscript Author Manuscript Author Manuscript Author Manuscript

Gene expression microarray analysis

MDA-MB-231 and HCC70 cells were treated with vehicle or 500 nM JQ1 for 72 hours and were processed for transcriptional profiling using Human Gene 2.0 ST expression microarray (Affymetrix). Cells were harvested and RNA was extracted with Trizol reagent (Ambion, 15596018) and treated with DNase I (Ambion, AM1906). RNA (50ng/μL) was delivered to the Gene Expression and Genotyping Core Facility at Case Western Reserve University. For each sample, 150 ng RNA was used to synthesize and label cDNA with biotin for hybridization to Human Gene 2.0 ST expression microarrays using the GeneChip WT Plus labeling kit and protocol, and the hybridized arrays were automatically stained and scanned with the Affymetrix standard stain and scan protocol. The microarray data were processed with RMA (robust multichip average algorithm) as implemented in Bioconductor package oligo (18) where background subtraction, quantile normalization and summarization (via median-polish) was accomplished. The top differentially expressed genes were identified using empirical Bayesian procedure of limma package (19). Multiple-testing correction was performed using the Benjamini-Hochberg method, thus providing false discovery rate (FDR) estimates per differentially expressed gene. The final list of differentially expressed genes was defined as those with p-values<0.05 and FDR<0.1. All data were submitted to GEO (GSE79332) using MIAME guidelines. The Reactome database (20) was used to identify the top five non-overlapping biological pathways regulated by BET inhibition in both cell lines with a p-value cutoff of 0.01. Violin and volcano plots were generated in R version 3.3.3 using RStudio version 1.0.136 (RStudio Inc). Two sample proportions tests were run in Stata SE 14 (StataCorp) with a significance cut-off of $p<0.05$.

Gene set enrichment analysis (GSEA)

GSEA (21) was utilized to determine whether *a priori* defined cell cycle- and breast cancer subtype-associated genes show statistically significant, concordant differences between vehicle- and JQ1-treated samples in HCC70 and MDA-MB-231 cell lines. The GSEA portal molecular signatures database (22) was used to define the cell cycle signatures. The subtype-associated gene sets were tabulated from Gray (23) and Bertucci (24) data sets as previously described (25). FDR-corrected p-values were considered to rank gene sets that had significant enrichment.

Western blot analysis

Western blot analysis was performed as previously described (25) using the following primary and secondary antibodies: LIN9 (Thermo Fisher, PA5-43640), β-actin (Sigma; A1978), Anti-rabbit IgG HRP-linked (Cell Signaling; 7074), and Anti-mouse IgG HRP-linked (Cell Signaling; 7076).

Gene-specific chromatin immunoprecipitation

ChIP-PCR was performed as previously described (26). MDA-MB-231 cells were treated for 24 hours with vehicle or 500 nM JQ1, and chromatin was immunoprecipitated with an anti-BRD4 specific antibody (Bethyl Laboratories, A301-985A50) or a control mouse IgG (Sigma, I5281). The following promoter-specific primers were used: FOXM1, forward 5′-GTAAGATGGAGGCGGTGTTG-3′ and reverse 5′-GGGTGGCCTACCTTCTTAGG-3′;

Author Manuscript Author Manuscript Author Manuscript Author Manuscript

E2F2, forward 5′-GACAATAGCAGGCACCCAGTA-3′ and reverse 5′-AGCACTGGATTGCGAGTCTG-3′; E2F8, forward 5′-TAGGAAGCACCCACCTGTTC-3′ and reverse 5′-GGGAGAAATCCAGGCATCTA-3′; LIN9, forward 5′-GGAACTGCAGGCTGTTTGTT-3′ and reverse 5′-GGGTTTCGGGAACTGTGAGT-3′; MYBL2, forward 5′-GTCTTCAAGTCCCAGCCAGT-3′ and reverse 5′-CCGGAATGTTAAGGAGCAAA-3′.

ChIP-seq

ChIP-seq was performed as previously described (26). Briefly, chromatin from MDA-MB-231 cells was immunoprecipitated with an anti-H3K27Ac specific antibody (Abcam, ab5079) or control mouse IgG (Sigma, I5281). Input and precipitated DNA were used to produce libraries and conduct high-throughput sequencing by the CWRU Genomics Sequencing Core. Sequences were quality-filtered using FASTX-Toolkit and aligned using Bowtie 2 (27). MACS (Model-based Analysis of ChIP-Seq) (28) was used to identify ChIP-enriched regions with a *p*-value enrichment threshold of 10^{-9}, and ROSE (Rank Ordering of Super-enhancers) software (17, 29) was used to identify enhancer regions. The enhancer element locations were then annotated using custom annotation scripts, jointly called *Grannotator* [manuscript under preparation]. Briefly, *Grannotator* combines genome-wide gene/transcript location information obtained from the UCSC Genome Browser and uses this information to annotate Granges (objects that contain the enhancer element locations). For each enhancer element, *Grannotator* provides the nearest 3′ and 5′ gene for both the forward and reverse strands in addition to the distance of the gene's transcription start site from the enhancer location. This information is then used to determine the gene most likely associated with an enhancer element. All data were submitted to GEO (GSE95222).

Bioinformatics

CBioPortal (30, 31) was used to identify the percent of breast cancer tumors with overexpressed (z score (RNA Seq V2 REM) ≥ 2.0) or amplified (GISTIC 2.0 score = 2) genes as well as genes that are correlated with *LIN9* in both the TCGA (32) and METABRIC (33, 34) datasets. Relapse free survival Kaplan-Meier curves in all breast cancer patients were generated with Kaplan-Meier plotter 2014 edition (35) and compared by the log-rank test. Patient groups corresponding to high/low tumor expression of *LIN9* were identified, resulting in an optimal expression cutoff of 111 to define the low (n=1127) and high (n=637) expression groups. To assess overall survival, gene expression data for the METABRIC dataset were retrieved from Oncomine (www.oncomine.com, Thermo Fisher Scientific). Samples (n = 1971) were segregated into high (upper 10^{th} percentile, n = 197) or low (remain 90^{th} percentile, n = 1774) groups based upon *LIN9* (probe ID ILMN_2137084) expression. The prognostic value of *LIN9* on 5-year overall survival in this dataset was analyzed by statistical comparison of Kaplan-Meier curves by the logrank test. 95% hazard ratios were calculated using a Cox regression model.

Statistical methods

Data are represented as mean values from three independent experiments performed in triplicate. Statistical analyses were performed using two-tailed Student's *t*-test or chi-squared test, and *p*-values less than 0.05 were considered statistically significant.

Author Manuscript Author Manuscript Author Manuscript Author Manuscript

RESULTS

Sustained BET activity is necessary for normal progression through mitosis

We previously reported that the loss of BET activity induces multinucleation, followed by two distinct terminal responses (apoptosis and senescence) irrespective of TNBC subtype (12). To confirm these outcomes, we treated two TNBC cell lines (MDA-MB-468 and HCC1143) with vehicle or the prototypical BETi, JQ1. After 72 hours, activation of caspases 3 and 7 was assessed to quantify the number of apoptotic cells. While both HCC1143 and MDA-MB-468 cells underwent apoptosis in response to JQ1, MDA-MB-468 cells had a greater apoptotic response compared to HCC1143 cells (Supplementary Fig. S1A). JQ1 also induced the expression of senescence-associated β-galactosidase (SA-βgal) activity in HCC1143 cells (Supplementary Fig. S1B), confirming that BETi induce senescence and/or apoptosis in TNBC, depending on the cell line examined.

Cells respond to mitotic catastrophe by activating senescence or apoptosis pathways (2, 3). Hence, the ability of BETi to induce these two responses as well as multinucleation suggested that sustained activity of BET proteins may be necessary for normal mitotic progression in TNBC cells. To assess the impact of losing BET function on mitosis, we used live cell imaging to track the fates of individual cells following treatment with JQ1. Both a primarily apoptotic (HCC38) and a primarily senescent (MDA-MB-231) cell line were observed over four days of vehicle or JQ1 exposure. Growth of HCC38 cells was completely arrested within 48 hours whereas MDA-MB-231 cells were initially more tolerant of JQ1 treatment (Fig. 1A). In both cases, when cells were tracked through their first mitosis following an initial six hours of drug treatment, JQ1 treatment significantly extended the time necessary for cells to complete mitosis (Fig. 1 B–D). In addition to initially increasing the duration of mitosis, JQ1 treatment had a profound effect on mitotic cell fate for both cell lines. The majority of JQ1-treated HCC38 cells died immediately following mitotic exit whereas only 6% of control-treated cells died during mitosis (Fig. 2A and B). In addition, 23% of JQ1-treated HCC38 cells died during mitosis compared to only 7% in vehicle-treated cells. Death during mitosis was also associated with an extended time traversing mitosis compared to cells that were completed mitosis (Fig. 2C). Similar to HCC38 cells, the MDA-MB-231 cell line experienced a large increase (~8 fold) in the percentage of cells that died immediately following mitosis with JQ1 treatment (Fig. 2D). While this cell line did not die during mitosis in response to JQ1, the drug caused cells to undergo a protracted interphase, meaning they exited mitosis and survived but never divided again, likely because they were entering senescence. Lastly, only ~6% of JQ1-treated MDA-MB-231 cells underwent a second cell division, and this was associated with a significant increase in post-mitotic timing (Fig. 2E). The induction of multinucleation (12), followed by apoptosis or senescence, and the induction of death either in, or immediately after, mitosis suggests that mitotic catastrophe is the primary mechanism of action of BETi efficacy in both models of TNBC.

BET activity is necessary for sustained expression of cell cycle-associated genes

To discern the molecular mechanism underlying the mitotic defects that occur with the loss of BET activity, we performed gene expression microarray analyses of cell lines that

Author Manuscript Author Manuscript Author Manuscript Author Manuscript

primarily undergo apoptosis (HCC70) or senescence (MDA-MB-231) in response to JQ1 (Fig. 3A–H). After 72 hours, the expression of 1271 genes in both cell lines was significantly altered in the same direction in response to JQ1 compared to vehicle (Fig. 3A; Supplementary Table S1). We found 149 (MDA-MB-231) and 51 (HCC70) Reactome pathways to be statistically significantly altered with BETi ($p<0.01$), of which the strongest enrichments were observed in cell cycle/mitosis and metabolism pathways (Fig. 3B). Gene set enrichment analysis (GSEA) using an established group of classifying genes for each stage of the cell cycle (22) revealed a significant ($p<0.05$) suppression of genes definitive for G2/M and M/G1 transitions in both cell lines following JQ1 treatment (Fig. 3C). JQ1-induced repression of eight genes that encode proteins involved in cell cycle regulation, mitosis, and/or cytokinesis was further confirmed by RT-qPCR in multiple TNBC cell lines (Fig. 3D–F; Fig. 4A). These genes were also downregulated in orthotopically xenografted tumors (MDA-MB-231 and MDA-MB-468) collected from mice treated with either vehicle or JQ1 (Fig. 3G; Fig. 4B and C). In addition, 14 of the 16 kinesins known to play critical roles in mitosis and cytokinesis in humans (36) were suppressed (Supplementary Table S1). Finally, in both MDA-MB-231 and HCC70 cells, there was a skewed JQ1-mediated downregulation of genes identified by SuperPath (37) as critical for mitosis ($p<<0.001$) (Fig. 3H). The reduced expression of mitosis-regulating genes in response to BETi in TNBC cells and tumors further supports a role for BET proteins in navigating the effective progression through mitosis in this disease.

BET inhibitors fail to induce a luminal differentiation signature

Breast cancer subtype switching has been observed with the manipulation of multiple transcription factors in breast cancer cell lines (25, 38). Given the roles of BET proteins as transcriptional modulators, we assessed whether their inhibition with JQ1 could induce a shift in breast cancer cell fate from the basal to luminal subtype. We assessed the potential for subtype switching by GSEA using the Gray (23) and Bertucci (24) gene sets that classify breast cancer cell line subtypes. Although the basal signature was diminished upon JQ1 treatment, TNBC cells failed to gain a luminal signature (Supplementary Fig. S2). Thus, while it has been suggested that a loss of BET activity results in the differentiation of TNBC cells (10), this genome-wide approach indicates BETi fail to induce full subtype switching, or luminal differentiation, of TNBC cell lines. These data further suggest shifts in breast cancer cell fate are unlikely to underlie the responsiveness of TNBC cells to BETi.

BET proteins directly modulate the mitotic transcriptional program

Further analysis of the microarray data described above revealed that the expression of nine genes encoding mitosis-controlling transcription factors was suppressed by BETi. Of these factors, four (*FOXM1*, *E2F8*, *LIN9*, and *MYBL2*) are associated with polyploidy (39–42), a key response we observed in TNBC cells following treatment with BETi (12). Another, *E2F2*, plays a critical role in the BETi response in liver cancer (43). These genes are rapidly repressed in MDA-MB-231 cells after just six hours of JQ1 treatment (Fig. 4A). The suppression of these genes by JQ1 was further confirmed in tumors from mice orthotopically xenografted with MDA-MB-231 or MDA-MB-468 cell lines (Fig. 4B and C). Notably, suppression of BET protein activity does not reduce all mitosis-regulating transcription factors. For example, expression of *LIN37*, a subunit of the MuvB core complex that

Author Manuscript Author Manuscript Author Manuscript Author Manuscript

regulates transcription of mitosis genes (1), was not suppressed with JQ1 treatment (Fig. 4A). An additional BETi currently being evaluated in clinical trials, I-BET762, also regulated the expression of these mitosis regulators in a similar manner, indicating the suppression of these genes is due to the inhibition of BET proteins and not off-target effects (Supplementary Fig. S3). To determine if the five genes are direct targets of BRD4, a BET family member, gene-specific chromatin immunoprecipitation (ChIP) assays were used. This approach revealed that BRD4 binds the promotor regions of all five genes and that BRD4 binding is significantly reduced with JQ1 exposure (Fig. 4D). This suggests that the mitotic disruption observed with the loss of BET protein activity may be due to the reduced expression of one or more of these factors.

To determine if these five mitosis-regulating transcription factors may be downstream effectors of BET proteins in TNBC, we used siRNA to simultaneously silence all five genes in MDA-MB-231 cells. We then examined whether the combined repression would phenocopy the BETi response by first examining the same cell cycle target genes evaluated above. The combined siRNAs effectively reduced the expression of all five factors (Supplementary Fig. S4A), as well as the expression of cell cycle genes (Supplementary Fig. S4B), in a manner similar to JQ1 treatment (Fig. 3D–F). Furthermore, expression of *CDKN1A*, which we previously reported increases with BETi treatment of TNBC cells (12), was also increased with the silencing of these five factors (Supplementary Fig. S4B). Most importantly, suppression of all five genes generated very large cells with multiple nuclei, a mitotic/cytokinetic defect that is comparable to that observed when BET proteins are inhibited (Supplementary Fig. S4C), indicating that the loss of these five factors can recapitulate BETi treatment.

BETi suppress mitosis transcription factors in the absence of super-enhancers

The increased sensitivity of cancer cells to BETi compared to non-transformed cells is proposed to result from the disassembly of super-enhancers (SEs) at oncogenes (16, 17). Thus, we assessed whether alterations in SEs may drive the response of the mitosis transcription factors identified above, and hence, the induction of mitotic catastrophe in TNBC. We generated a SE map of MDA-MB-231 cells using H3K27Ac ChIP-seq and compared the list of SE-containing genes to those regulated by JQ1. In MDA-MB-231 cells, 1038 genes have putative SEs, accounting for 3% of all genes, whereas 8.6% of genes whose expression is altered by JQ1 contain super-enhancers ($p<0.01$) (Fig. 5A). This confirms prior reports indicating that BETi-regulated genes are enriched for SEs when interrogating the full complement of protein coding genes (16, 17). When examining the subset of 599 genes identified as mitosis-associated genes by SuperPath (37), a larger percentage of these genes contain a SE (~10%, $p<0.005$), yet there was no enrichment of SEs at mitosis genes regulated by JQ1 compared to those that are not. Thus, while mitosis-associated genes generally are more likely to contain a SE than other genes, the presence of a SE does not dictate their response to BETi. Across the genome, genes that contain a SE undergo greater repression by BETi than genes that lack a SE (Fig. 5B). However, when selectively examining mitosis-associated genes, the extent of repression of these genes is independent of the presence or absence of a SE (Fig. 5C). Lastly, we found no correlation between the

Author Manuscript Author Manuscript Author Manuscript Author Manuscript

strength of a gene's enhancer score, defined by H3K27Ac presence under basal conditions, with its extent of repression following JQ1 treatment (Fig. 5D).

To determine if any of the five mitosis-regulating transcription factors we identified as early responders to BETi (*FOXM1*, *E2F2*, *E2F8*, *LIN9*, and *MYBL2*) are associated with SEs, we examined the ChIP-seq binding profiles for H3K27Ac at these genes. None of these genes have putative SEs (Fig. 5D and E), even though a SE at *MYC* is readily detected. We also examined a dataset of BRD4 binding profiles in a larger panel of TNBC cell lines compiled by Shu *et al*. and confirmed in this additional dataset that these genes lacked SEs. Together, these data indicate that disruption of SEs is unlikely to be the primary mechanism by which BETi suppress mitosis-regulating transcription factors. Thus SE disassembly is not responsible for the induction of mitotic catastrophe in response to BETi in TNBC. Rather, mitotic catastrophe occurs as a result of the direct suppression of master regulators of mitosis through the loss of typical BRD4 binding to the promotor regulatory regions of these genes.

LIN9 is a key downstream effector of BET proteins

Of the five transcription factors evaluated above, three interact to modulate cell cycle progression and prevent entry into senescence. LIN9 is one of five subunits of the MuvB complex that works with FOXM1 and B-MYB (the protein product of *MYBL2*) to drive expression of critical mitosis genes and ensure proper progression through the cell cycle (44). To assess whether reduced expression of these three genes is responsible for the observed mitotic defect that occurs with the loss of BET activity, or if *E2F2* and *E2F8* are also necessary, we simultaneously silenced the expression of *FOXM1*, *LIN9*, and *MYBL2* using siRNA transfection. After five days, all three genes remained suppressed. More importantly, the same cell cycle target genes suppressed by the set of five factors were also inhibited with the loss of just *FOXM1*, *LIN9*, and *MYBL2*. Silencing these three factors also caused the cells to become large and multinucleated (Supplementary Fig. S5A and B), indicating that suppression of *E2F2* and *E2F8* were unnecessary for the mitotic response. We then sought to determine which BET protein(s) is necessary for the expression of *FOXM1*, *LIN9*, and *MYBL2*. We used individual and pairwise siRNA transfections to silence *BRD2*, *BRD3*, and/or *BRD4* for 72 hours. Only simultaneous loss of *BRD2* and *BRD4* suppressed expression of *FOXM1*, *LIN9*, and *MYBL2* (Supplementary Fig. S5C and D). These data further affirm the selectivity of BETi in controlling the expression of these three genes. Notably, we also found that silencing either *BRD2* or *BRD4* reduces *BRD3* expression, and this suppression is further enhanced when *BRD2* and *BRD4* are silenced together (Supplementary Fig. S5C and D). To our knowledge, this is the first time BRD2 and BRD4 have been shown to be necessary for sustained *BRD3* expression.

We then determined if loss of just one of the mitosis-associated transcription factors is sufficient for mediating the BETi response in TNBC by using siRNAs individually targeting *FOXM1*, *LIN9*, or *MYBL2*. As controls, we also individually silenced *E2F2* or *E2F8*. After five days, expression of all targeted genes was reduced (Fig. 6A; Supplementary Fig. S6A). However, only loss of *LIN9* altered the expression of cell cycle target genes in the same direction as JQ1 (Fig. 6B; Supplementary Fig. S6B). In addition, silencing *LIN9* induced

Author Manuscript Author Manuscript Author Manuscript Author Manuscript

significant multinucleation that is comparable to that observed with JQ1 treatment (Fig. 6C). This suggests that LIN9 is a principle target of BET proteins that is necessary for maintaining mitotic progression.

To assess the clinical significance of LIN9 in human breast cancer, we interrogated publically available datasets for changes in *LIN9* copy number or expression and found *LIN9* is amplified or overexpressed in 24–29% of all breast tumors in the TCGA (32) and METABRIC (33, 34) datasets. In the basal-like subset of breast cancers, *LIN9* is amplified and/or overexpressed in 66% of TCGA samples (19% amplified, 65% overexpressed). We assessed BETi-induced apoptosis in four TNBC cell lines (MDA-MB-231, HCC1143, MDA-MB-468, and BT549) and found there is no difference in the extent of apoptosis in cells with amplified vs. non-amplified but overexpressed LIN9 (data not shown). In contrast, other subunits of the MuvB complex are amplified or overexpressed in less than 5% of all breast cancers and less than 20% of basal-like cancers. Kaplan-Meier survival analysis revealed high expression of *LIN9* is correlated with lower relapse-free (Fig. 6D) and overall survival (Supplementary Fig. S7) rates in all breast cancer patients. Together, these data implicate LIN9 as a driver of breast cancer, in general, and of TNBC, specifically. Given the frequent amplification of *LIN9* in TNBC, it was possible that the absence of a SE at the *LIN9* locus was due to DNA-content normalization used in the analysis of H3K27Ac ChIP-seq data. However, the Cancer Cell Line Encyclopedia (45) revealed that *LIN9* is not amplified in MDA-MB-231 cells. Further indicating that our approach would not eclipse SE assignments due to amplification of a genomic locus, the *MYC* gene was identified as having a SE even though *MYC* is highly amplified in these cells. Thus, *LIN9* amplification often leads to its overexpression in the absence of a canonical SE and this expression can be suppressed with BETi.

To infer the global potential of modulating *LIN9* expression as a mediator of BETi, we identified genes whose expression is highly correlated (Pearson's coefficient $r \geq 0.5$) with *LIN9* in breast cancer samples from TCGA and determined if these genes may be particularly sensitive to BETi (Supplementary Table S2), reasoning this would implicate *LIN9* as being upstream of these correlated genes. This analysis revealed that most genes whose expression does not correlate with *LIN9* ($r<0.5$) in breast cancer samples are also unresponsive to BETi in MDA-MB-231 cells (Fig. 6E). In stark contrast, the majority of genes whose expression is highly correlated with *LIN9* in breast cancer samples ($r \geq 0.5$) are suppressed by BETi in TNBC cells, with correlated genes being on average 2.5–3.2 fold more repressed by BETi than non-correlated genes (Fig. 6F). Several genes whose expression correlates with *LIN9* are co-amplified with this gene. To determine if BETi was simply modulating expression of genes within the *LIN9* amplicon, we subdivided the group of *LIN9*-correlated genes into those that reside on chromosome 1q and those that do not. While a subset of genes on 1q are repressed by BETi, most are not. Furthermore, most of the *LIN9*-correlated genes that do not reside in this region are generally much more suppressed by BETi (Fig. 6E). As a member of the MuvB complex, LIN9 interacts with 1,379 genes across the genome in HeLa cells (44). To determine if BETi responsive genes can bind to LIN9/MuvB, we interrogated this dataset and found that 27.4% of genes reported to bind LIN9/MuvB are also regulated by JQ1 in TNBC cells. In contrast, only 8.9% of non-MuvB

Author Manuscript Author Manuscript Author Manuscript Author Manuscript

bound genes are modulated by JQ1 ($p<0.01$, Fig. 6G). Together, these data indicate LIN9 is downstream of BET proteins and a major mediator of BETi in TNBC cells.

DISCUSSION

Identifying new therapeutic targets for TNBC is essential for improving outcomes of patients with this disease. Using genetic and pharmacologic approaches, it is well-established that the activity of BET proteins is essential for TNBC cell growth, *in vitro* and *in vivo* (9–13). However, the mechanism of action of BETi in this disease has not been fully elucidated. To ensure effective clinical utilization of these drugs, it is critical to develop a detailed understanding of their mechanisms of action. Such information will be key for predicting which tumors are likely to respond and for the rational selection of drug combinations. We recently showed that BETi produce two distinct responses, apoptosis and senescence, and these are preceded by multinucleation, indicating BETi induce mitotic dysfunction (12). Here, we report that BETi repress TNBC growth by inducing mitotic catastrophe. In 2012, the International Nomenclature on Cell Death defined mitotic catastrophe as an onco-suppressive mechanism that occurs in response to aberrant mitosis, coincides with mitotic arrest, and induces any of three irreversible cell fates: death during mitosis, apoptosis following mitotic exit, or senescence (3, 46). The study described herein provides several lines of evidence substantiating the role of mitotic catastrophe in the BETi response of TNBC cells. First, we found BETi suppress a large number of mitosis-regulating genes, including several (*KIF20A, AURKA*, *AURKB*, and *FOXM1)* whose loss is known to cause mitotic catastrophe (3). Supporting the expression studies herein, Borbely *et al*. also recently reported that BETi repress cell cycle gene expression in breast cancer (13). Second, we found suppression of BET activity increases the amount of time cells spend traversing mitosis with many becoming multinucleated, processes that are also associated with mitotic catastrophe (3). Lastly, direct evidence of BETi-induced mitotic catastrophe was observed when individual cells were followed through mitosis. Live cell imaging revealed JQ1 greatly increases the number of cells that die during mitosis as well as the number that exit mitosis and die soon thereafter. It is well-known that mitotic catastrophe induces senescence or apoptosis, and this depends on the individual cell line (3). Both outcomes were observed in response to BETi but were cell line-specific (12). Together, these data indicate a loss of BET activity conveyed by BETi induces mitotic catastrophe which leads to apoptosis and senescence in TNBC.

BETi induce apoptosis and senescence in TNBC while having no evident effect on the normal mammary gland (12). This preferential impact on cancer cells compared to non-transformed cells has been attributed to the disruption of SEs (16, 17, 47). BRD4 disproportionately binds to SEs, with about 30–40% of all bound BRD4 located at these specialized regions of the chromatin (16, 17). Like other co-activators, BRD4 exhibits cooperative binding. As a result, BRD4 inhibition causes greater downregulation of SE-associated genes than typical enhancer-associated genes (16, 17). We now report that inhibition of BET proteins also leads to extensive dysregulation of cell cycle genes that are particularly active in cancer. Besides being more sensitive to the disruption of SEs, cancer cells are also more susceptible to mitotic catastrophe than non-transformed cells (48). Thus, we pose an alternative explanation for the cancer-specificity of BETi: specifically, these

Author Manuscript Author Manuscript Author Manuscript Author Manuscript

drugs induce mitotic catastrophe, at least in TNBC, and, because cancer cells are particularly prone to this process, they initiate cell death or senescence pathways. Notably, none of the genes we found to be functionally involved in the response of TNBC to BETi are associated with SEs in MDA-MB-231 cells or a larger panel of TNBC cell lines (10). This suggests disruption of SEs may not be essential for the inhibition of TNBC growth observed when BET protein activity is suppressed. Indeed, we found that loss of a group of mitosis-regulating transcription factors phenocopied the effects of BET suppression and none of those genes contain a conventionally-defined SE.

The analysis described herein revealed that suppression of BET activity downregulates *LIN9* as well as four additional mitosis-regulating transcription factors within six hours of treatment. Of the five BETi-regulated transcription factors we investigated, only individually silencing *LIN9* mimics BETi treatment by repressing mitosis-associated genes and inducing multinucleation. LIN9 is reported to contribute to a variety of processes, including embryonic development, progression through G2-phase, mitosis, and cytokinesis (41, 49, 50), and is a component of the Mammaprint breast cancer gene signature that predicts metastasis (51). Along with LIN37, LIN52, LIN54, and RBBP4, LIN9 is a subunit of the MuvB complex (1). During S phase, the MuvB complex interacts with B-MYB, and together they drive the expression of late S-phase genes (44, 52). They then recruit FOXM1 to the chromatin during G2 phase (52). B-MYB is phosphorylated and subsequently degraded by the proteasome (44), while FOXM1 is phosphorylated and activated (53). Phosphorylated FOXM1 and the MuvB complex remain bound to the DNA and regulate expression of genes important for the G2/M transition and successful completion of mitosis, including *AURKA*, *AURKB*, *PLK1*, and *KIF20A* (39, 49, 52), all of which are also suppressed with BETi treatment. In addition, six mitotic kinesins (KIF4A, KIF23, KIF2C, KIF14, KIFC1, and KIF20A) and two microtubule-associated non-motor proteins (PRC1 and CEP55) that have known functions in mitosis and cytokinesis are direct targets of MuvB, B-MYB, and FOXM1 in breast cancer (54). Expression of genes encoding these proteins as well as eight additional mitotic kinesins (36) were downregulated following BETi treatment. Prior studies have shown that loss of *LIN9* expression produces polyploid cells with aberrant nuclei and induces senescence (49, 55). Thus, data presented herein not only confirm the impact of LIN9 on mitosis, but also implicate LIN9 as an intermediate between BET proteins and effective mitosis in TNBC.

Using the TCGA and METABRIC datasets, we found that *LIN9* is amplified or overexpressed in 24–29% of all breast tumors and in 66% of basal-like tumors. High expression of *LIN9* is also associated with poor survival of breast cancer patients. Supporting a role for LIN9 in mediating the effects of BET proteins, we found that genes highly correlated with LIN9 are more susceptible to BET suppression than those that are not. Furthermore, genes harboring a MuvB binding site, indicative of LIN9 association, were also more likely to be suppressed by JQ1. Together, these data suggest loss of LIN9 expression in response to BETi initiates a cascade of events wherein many cell cycle-regulated genes are suppressed, mitosis is disrupted, and cells either become multinucleated, die, or enter a prolonged interphase (G_0). These results also argue that breast cancers with amplified or overexpressed *LIN9* may be more susceptible to BET inhibition and this

Author Manuscript Author Manuscript Author Manuscript Author Manuscript

possibility could be evaluated in clinical trials currently underway examining the efficacy of BETi in TNBC patients.

In summary, direct BET protein binding is necessary to sustain expression of *LIN9* as well as several additional mitosis-regulating transcription factors in TNBC. Loss of BET protein activity through the use of BETi suppresses key cell cycle and mitosis genes causing mitotic catastrophe. Reduced expression of *LIN9* alone can mimic the effects of BET protein suppression, suggesting that it is a primary mediator of BETi. Notably, *LIN9*, as well as genes encoding the other mitosis-associated transcription factors evaluated in this study, lack super-enhancers, indicating that disruption of such elements is unnecessary for the mitotic dysfunction observed with these inhibitors. Given the high rate of overexpression of *LIN9* in breast cancers, these data suggest LIN9 may be a key vulnerability in breast cancers that can be targeted with BETi. They further suggest BETi may be particularly effective when combined with additional agents that increase cancer cell sensitivity to mitotic dysfunction.

Supplementary Material

Refer to Web version on PubMed Central for supplementary material.

Acknowledgments

We thank James Bradner for providing JQ1. We also thank Alina Saiakhova for her expert guidance on identifying super-enhancers and Jessica Vespoli (Ohio State) for her assistance with the analysis of data acquired using live cell imaging. The following Core Facilities of the Case Comprehensive Cancer Center also supported this work: Gene Expression and Genotyping, Athymic Animal and Xenograft, and Genomics Sequencing Core.

Financial support:

J.M. Sahni: T32CA059366, F99CA212460

S.S. Gayle: T32CA059366

B.M. Webb: T32GM008803

N.A. Restrepo: R25TCA094186

G. Bebek: KL2TR000440

M.K. Summers: RO1GM112895, RO1GM108743

R.A. Keri: RO1CA154384, RO1CA206505

References

1. Nath S, Ghatak D, Das P, Roychoudhury S. Transcriptional control of mitosis: deregulation and cancer. Front Endocrinol. 2015; 6:60.
2. Denisenkoa TV, Sorokina IV, Gogvadze V, Zhivotovsky B. Mitotic catastrophe and cancer drug resistance: A link that must to be broken. Drug Resist Updat. 2016; 24:1–12. [PubMed: 26830311]
3. Vitale I, Galluzzi L, Castedo M, Kroemer G. Mitotic catastrophe: a mechanism for avoiding genomic instability. Nat Rev Mol Cell Biol. 2011; 12:385–92. [PubMed: 21527953]
4. Roninson IB, Broude EV, Chang B-D. If not apoptosis, then what? Treatment-induced senescence and mitotic catastrophe in tumor cells. Drug Resist Updat. 2001; 4:303–13. [PubMed: 11991684]

Author Manuscript Author Manuscript Author Manuscript Author Manuscript

5. Jiang L, Siu MKY, Wong OGW, Tam K-F, Lu X, Lam EW-F, et al. iASPP and chemoresistance in ovarian cancers: effects on paclitaxel-mediated mitotic catastrophe. Clin Cancer Res. 2011; 17:6924–33. [PubMed: 21926165]
6. Nitta M, Kobayashi O, Honda S, Hirota T, Kuninaka S, Marumoto T, et al. Spindle checkpoint function is required for mitotic catastrophe induced by DNA-damaging agents. Oncogene. 2004; 23:6548–58. [PubMed: 15221012]
7. Vakifahmetoglu H, Olsson M, Zhivotovsky B. Death through a tragedy: Mitotic catastrophe. Cell Death Differ. 2008; 15:1153–62. [PubMed: 18404154]
8. Jitariu A-A, Cîmpean AM, Ribatti D, Raica M. Triple negative breast cancer: the kiss of death. Oncotarget. 2017
9. Shi J, Wang Y, Zeng L, Wu Y, Deng J, Zhang Q, et al. Disrupting the interaction of BRD4 with diacetylated Twist suppresses tumorigenesis in basal-like breast cancer. Cancer Cell. 2014; 25:210–25. [PubMed: 24525235]
10. Shu S, Lin CY, He HH, Witwicki RM, Tabassum DP, Roberts JM, et al. Response and resistance to BET bromodomain inhibitors in triple-negative breast cancer. Nature. 2016; 529:413–7. [PubMed: 26735014]
11. da Motta LL, Ledaki I, Purshouse K, Haider S, De Bastiani MA, Baban D, et al. The BET inhibitor JQ1 selectively impairs tumour response to hypoxia and downregulates CA9 and angiogenesis in triple negative breast cancer. Oncogene. 2016
12. Sahni JM, Gayle SS, Weber-Bonk KL, Cuellar Vite L, Yori JL, Webb B, et al. Bromodomain and extraterminal protein inhibition blocks growth of triple-negative breast cancers through the suppression of Aurora kinases. J Biol Chem. 2016; 291:23756–68. [PubMed: 27650498]
13. Borbely G, Haldosen L-A, Dahlman-Wright K, Zhao C. Induction of USP17 by combining BET and HDAC inhibitors in breast cancer cells. Oncotarget. 2015; 6:33623–35. [PubMed: 26378038]
14. Filippakopoulos P, Qi J, Picaud S, Shen Y, Smith WB, Fedorov O, et al. Selective inhibition of BET bromodomains. Nature. 2010; 468:1067–73. [PubMed: 20871596]
15. Shi J, Vakoc CR. The mechanisms behind the therapeutic activity of BET bromodomain inhibition. Mol Cell. 2014; 54:728–36. [PubMed: 24905006]
16. Chapuy B, McKeown MR, Lin CY, Monti S, Roemer MGM, Qi J, et al. Discovery and characterization of super-enhancer-associated dependencies in diffuse large B cell lymphoma. Cancer Cell. 2013; 24:777–90. [PubMed: 24332044]
17. Lovén J, Hoke HA, Lin CY, Lau A, Orlando DA, Vakoc CR, et al. Selective inhibition of tumor oncogenes by disruption of super-enhancers. Cell. 2013; 153:320–34. [PubMed: 23582323]
18. Carvalho BS, Irizarry RA. A framework for oligonucleotide microarray preprocessing. Bioinformatics. 2010; 26:2363–7. [PubMed: 20688976]
19. Ritchie ME, Phipson B, Wu D, Hu Y, Law CW, Shi W, et al. limma powers differential expression analyses for RNA-sequencing and microarray studies. Nucleic Acids Res. 2015; 43:e47. [PubMed: 25605792]
20. Joshi-Tope G, Gillespie M, Vastrik I, D'Eustachio P, Schmidt E, de Bono B, et al. Reactome: a knowledgebase of biological pathways. Nucleic Acids Res. 2005; 33:D428–32. [PubMed: 15608231]
21. Subramanian A, Tamayo P, Mootha VK, Mukherjee S, Ebert BL, Gillette MA, et al. Gene set enrichment analysis: a knowledge-based approach for interpreting genome-wide expression profiles. Proc Natl Acad Sci USA. 2005; 102:15545–50. [PubMed: 16199517]
22. Liberzon A, Subramanian A, Pinchback R, Thorvaldsdóttir H, Tamayo P, Mesirov JP. Molecular signatures database (MSigDB) 3.0. Bioinformatics. 2011; 27:1739–40. [PubMed: 21546393]
23. Neve RM, Chin K, Fridlyand J, Yeh J, Baehner FL, Fevr T, et al. A collection of breast cancer cell lines for the study of functionally distinct cancer subtypes. Cancer Cell. 2006; 10:515–27. [PubMed: 17157791]
24. Charafe-Jauffret E, Ginestier C, Monville F, Finetti P, Adélaïde J, Cervera N, et al. Gene expression profiling of breast cell lines identifies potential new basal markers. Oncogene. 2006; 25:2273–84. [PubMed: 16288205]

Author Manuscript Author Manuscript Author Manuscript Author Manuscript

25. Bernardo GM, Bebek G, Ginther CL, Sizemore ST, Lozada KL, Miedler JD, et al. FOXA1 represses the molecular phenotype of basal breast cancer cells. Oncogene. 2013; 32:554–63. [PubMed: 22391567]
26. Yori JL, Johnson E, Zhou G, Jain MK, Keri RA. Kruppel-like factor 4 inhibits epithelial-to-mesenchymal transition through regulation of E-cadherin gene expression. J Biol Chem. 2010; 285:16854–63. [PubMed: 20356845]
27. Langmead B, Salzberg SL. Fast gapped-read alignment with Bowtie 2. Nat Methods. 2012; 9:357–9. [PubMed: 22388286]
28. Zhang Y, Liu T, Meyer CA, Eeckhoute J, Johnson DS, Bernstein BE, et al. Model-based analysis of ChIP-Seq (MACS). Genome Biol. 2008; 9:R137. [PubMed: 18798982]
29. Whyte WA, Orlando DA, Hnisz D, Abraham BJ, Lin CY, Kagey MH, et al. Master transcription factors and mediator establish super-enhancers at key cell identity genes. Cell. 2013; 153:307–19. [PubMed: 23582322]
30. Gao J, Aksoy BA, Dogrusoz U, Dresdner G, Gross B, Sumer SO, et al. Integrative analysis of complex cancer genomics and clinical profiles using the cBioPortal. Sci Signal. 2013; 6:pl1. [PubMed: 23550210]
31. Cerami E, Gao J, Dogrusoz U, Gross BE, Sumer SO, Aksoy BA, et al. The cBio cancer genomics portal: an open platform for exploring multidimensional cancer genomics data. Cancer Discov. 2012; 2:401–4. [PubMed: 22588877]
32. Ciriello G, Gatza ML, Beck AH, Wilkerson MD, Rhie SK, Pastore A, et al. Comprehensive Molecular Portraits of Invasive Lobular Breast Cancer. Cell. 2015; 163:506–19. [PubMed: 26451490]
33. Curtis C, Shah SP, Chin S-F, Turashvili G, Rueda OM, Dunning MJ, et al. The genomic and transcriptomic architecture of 2,000 breast tumours reveals novel subgroups. Nature. 2012; 486:346–52. [PubMed: 22522925]
34. Pereira B, Chin S-F, Rueda OM, Vollan H-KM, Provenzano E, Bardwell HA, et al. The somatic mutation profiles of 2,433 breast cancers refines their genomic and transcriptomic landscapes. Nat Commun. 2016; 7:11479. [PubMed: 27161491]
35. Győrffy B, Lanczky A, Eklund AC, Denkert C, Budczies J, Li Q, et al. An online survival analysis tool to rapidly assess the effect of 22,277 genes on breast cancer prognosis using microarray data of 1,809 patients. Breast Cancer Res Treat. 2010; 123:725–31. [PubMed: 20020197]
36. Rath O, Kozielski F. Kinesins and cancer. Nat Rev Cancer. 2012; 12:527–39. [PubMed: 22825217]
37. Belinky F, Nativ N, Stelzer G, Zimmerman S, Stein TI, Safran M, et al. PathCards: Multi-source consolidation of human biological pathways. Database. 2015; 2015
38. Chu IM, Michalowski AM, Hoenerhoff M, Szauter KM, Luger D, Sato M, et al. GATA3 inhibits lysyl oxidase-mediated metastases of human basal triple-negative breast cancer cells. Oncogene. 2012; 31:2017–27. [PubMed: 21892208]
39. Wang I-C, Chen Y-J, Hughes D, Petrovic V, Major ML, Park HJ, et al. Forkhead box M1 regulates the transcriptional network of genes essential for mitotic progression and genes encoding the SCF (Skp2-Cks1) ubiquitin ligase. Mol Cell Biol. 2005; 25:10875–94. [PubMed: 16314512]
40. Pandit SK, Westendorp B, Nantasanti S, van Liere E, Tooten PCJ, Cornelissen PWA, et al. E2F8 is essential for polyploidization in mammalian cells. Nat Cell Biol. 2012; 14:1181–91. [PubMed: 23064264]
41. Esterlechner J, Reichert N, Iltzsche F, Krause M, Finkernagel F, Gaubatz S. LIN9, a subunit of the DREAM complex, regulates mitotic gene expression and proliferation of embryonic stem cells. PLoS One. 2013; 8:e62882. [PubMed: 23667535]
42. Tarasov KV, Tarasova YS, Tam WL, Riordon DR, Elliott ST, Kania G, et al. B-MYB is essential for normal cell cycle progression and chromosomal stability of embryonic stem cells. PLoS One. 2008; 3:e2478. [PubMed: 18575582]
43. Hong SH, Eun JW, Choi SK, Shen Q, Choi WS, Han J-W, et al. Epigenetic reader BRD4 inhibition as a therapeutic strategy to suppress E2F2-cell cycle regulation circuit in liver cancer. Oncotarget. 2016; 7:32628–40. [PubMed: 27081696]
44. Sadasivam S, Duan S, DeCaprio JA. The MuvB complex sequentially recruits B-Myb and FoxM1 to promote mitotic gene expression. Genes Dev. 2012; 26:474–89. [PubMed: 22391450]

Author Manuscript Author Manuscript Author Manuscript Author Manuscript

45. Barretina J, Caponigro G, Stransky N, Venkatesan K, Margolin AA, Kim S, et al. The Cancer Cell Line Encyclopedia enables predictive modelling of anticancer drug sensitivity. Nature. 2012; 483:603–7. [PubMed: 22460905]

46. Galluzzi L, Vitale I, Abrams JM, Alnemri ES, Baehrecke EH, Blagosklonny MV, et al. Molecular definitions of cell death subroutines: recommendations of the Nomenclature Committee on Cell Death 2012. Cell Death Differ. 2012; 19:107–20. [PubMed: 21760595]

47. Dawson MA, Prinjha RK, Dittmann A, Giotopoulos G, Bantscheff M, Chan W-I, et al. Inhibition of BET recruitment to chromatin as an effective treatment for MLL-fusion leukaemia. Nature. 2011; 478:529–33. [PubMed: 21964340]

48. Janssen A, Kops GJPL, Medema RH. Elevating the frequency of chromosome mis-segregation as a strategy to kill tumor cells. Proc Natl Acad Sci USA. 2009; 106:19108–13. [PubMed: 19855003]

49. Reichert N, Wurster S, Ulrich T, Schmitt K, Hauser S, Probst L, et al. Lin9, a subunit of the mammalian DREAM complex, is essential for embryonic development, for survival of adult mice, and for tumor suppression. Mol Cell Biol. 2010; 30:2896–908. [PubMed: 20404087]

50. Osterloh L, von Eyss B, Schmit F, Rein L, Hübner D, Samans B, et al. The human synMuv-like protein LIN-9 is required for transcription of G2/M genes and for entry into mitosis. EMBO J. 2007; 26:144–57. [PubMed: 17159899]

51. van ’t Veer LJ, Dai H, van de Vijver MJ, He YD, Hart AAMH, Mao M, et al. Gene expression profiling predicts clinical outcome of breast cancer. Nature. 2002; 415:530–6. [PubMed: 11823860]

52. Litovchick L, Sadasivam S, Florens L, Zhu X, Swanson SK, Velmurugan S, et al. Evolutionarily conserved multisubunit RBL2/p130 and E2F4 protein complex represses human cell cycle-dependent genes in quiescence. Mol Cell. 2007; 26:539–51. [PubMed: 17531812]

53. Laoukili J, Alvarez M, Meijer LAT, Stahl M, Mohammed S, Kleij L, et al. Activation of FoxM1 during G2 requires cyclin A/Cdk-dependent relief of autorepression by the FoxM1 N-terminal domain. Mol Cell Biol. 2008; 28:3076–87. [PubMed: 18285455]

54. Wolter P, Hanselmann S, Pattschull G, Schruf E, Gaubatz S. Central spindle proteins and mitotic kinesins are direct transcriptional targets of MuvB, B-MYB and FOXM1 in breast cancer cell lines and are potential targets for therapy. Oncotarget. 2017; 8:11160–72. [PubMed: 28061449]

55. Hauser S, Ulrich T, Wurster S, Schmitt K, Reichert N, Gaubatz S. Loss of LIN9, a member of the DREAM complex, cooperates with SV40 large T antigen to induce genomic instability and anchorage-independent growth. Oncogene. 2012; 31:1859–68. [PubMed: 21860417]

Author Manuscript Author Manuscript Author Manuscript Author Manuscript

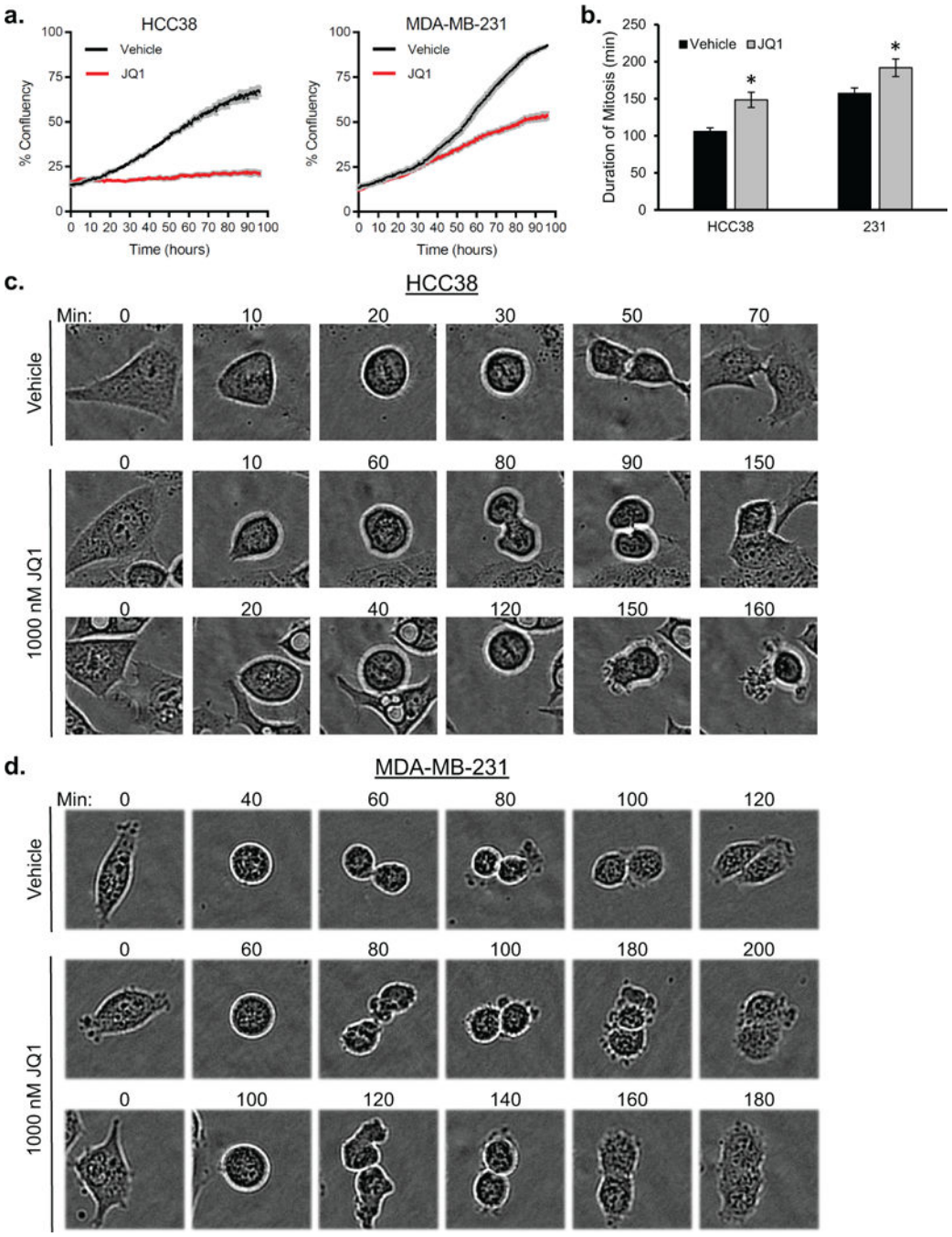

Figure 1. Sustained BET activity is necessary for timely progression through mitosis

HCC38 and MDA-MB-231 cells were treated with vehicle or 1000 nM JQ1 and observed via live-cell imaging for 96 hours. (**A**) Average percent confluency of HCC38 (left) and MDA-MB-231 (right) cells over time. Data are means ± SEM. (**B**) Quantitation of the length of time required by individual TNBC cells to complete mitosis six hours after the addition of vehicle or JQ1. Data are means ± SEM (*=$p<0.05$ compared to vehicle). (**C** and **D**) Representative live-cell images (20×) of HCC38 (**C**) and MDA-MB-231 (**D**) cells treated with vehicle or 1000 nM JQ1. Numbers indicate minutes following the initiation of mitosis.

Author Manuscript Author Manuscript Author Manuscript Author Manuscript

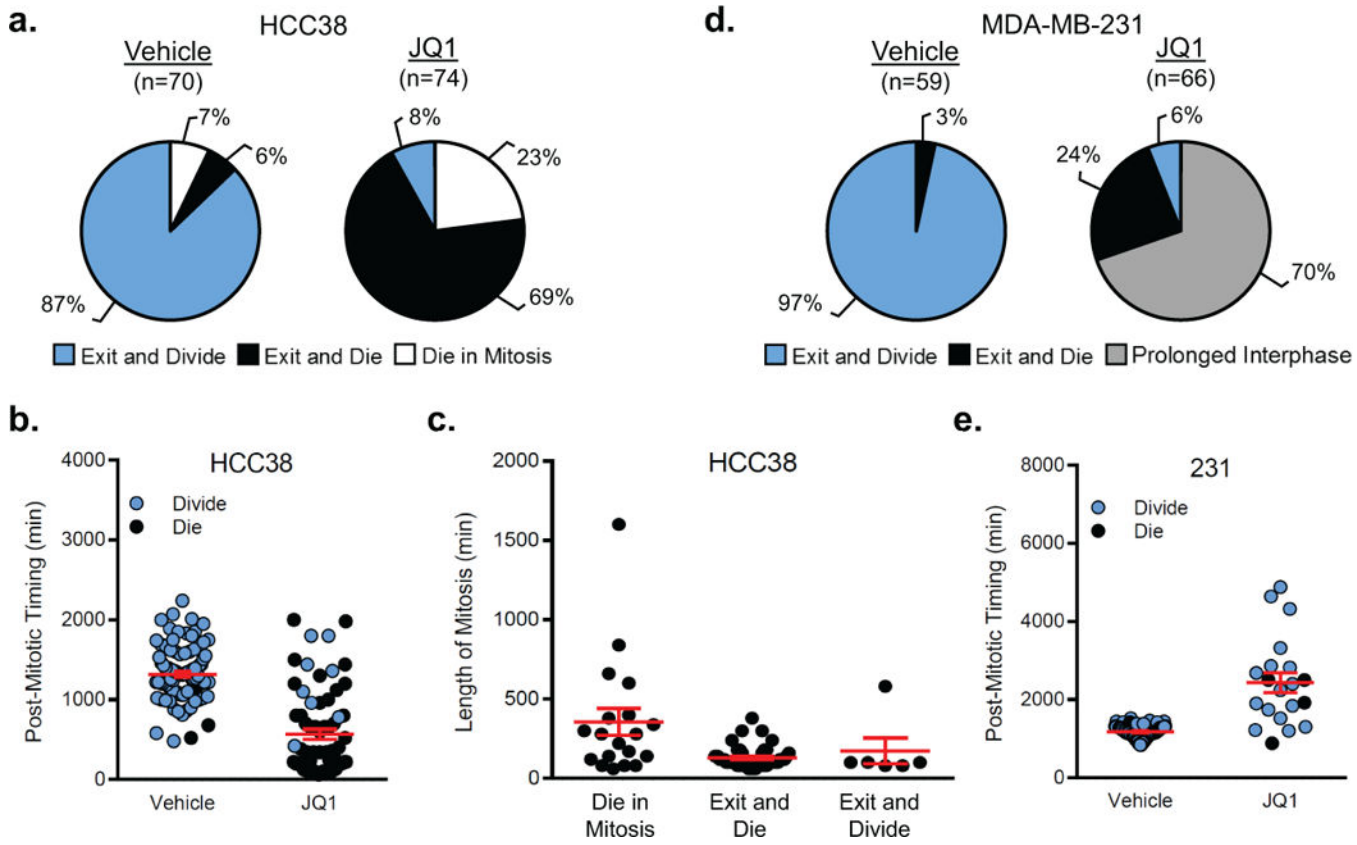

Figure 2. BET inhibitors promote mitosis-associated death or prolonged interphase

(**A**) Pie chart showing the percentage of vehicle- and JQ1-treated HCC38 cells that underwent different mitosis-associated cell fates: exit and divide (blue), exit and die (black), or die in mitosis (white). Vehicle *versus* JQ1 for all three outcomes, $p<<0.001$. (**B**) Quantitation of the length of time for HCC38 cells to divide again (blue dots) or die (black dots) following mitotic exit. $p<0.05$ compared to vehicle. (**C**) Comparison of the duration of mitosis of individual JQ1-treated HCC38 cells that die in mitosis, exit mitosis and die, or exit mitosis and divide. Die in Mitosis *versus* Exit and Die, $p<0.05$. (**D**) Pie chart showing the percentage of vehicle- and JQ1-treated MDA-MB-231 cells that underwent different post-mitotic cell fates: exit and divide (blue), exit and die (black), or prolonged interphase (grey). Vehicle *versus* JQ1 for all three outcomes, $p<<0.001$. (**E**) Quantitation of the length of time for MDA-MB-231 cells to divide again (blue dots) or die (black dots) following mitotic exit. $p<0.05$ compared to vehicle. For all graphs, each dot represents an individual cell, and red lines are mean ± SEM.

Author Manuscript Author Manuscript Author Manuscript Author Manuscript

a.

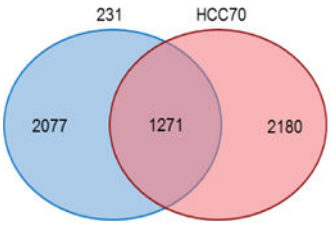

b.

MDA-MB-231		
Pathway	**p-value**	**q-value**
Mitotic Prometaphase	1.7E-23	6.2E-21
S Phase	2.7E-19	4.9E-17
Signaling by Rho GTPases	1.9E-10	1.1E-8
Mitotic G2-G2/M Phases	3.8E-10	2.0E-8
Kinesins	3.1E-06	9.8E-5

HCC70		
Pathway	**p-value**	**q-value**
Metabolism	2.9E-06	3.0E-3
Cell Cycle, Mitotic	3.4E-05	0.01
Assembly of the Primary Cilium	5.1E-05	0.01
Apoptotic Execution Phase	0.00014	0.03
Non-Integrin Membrane-ECM Interactions	0.00022	0.03

c.

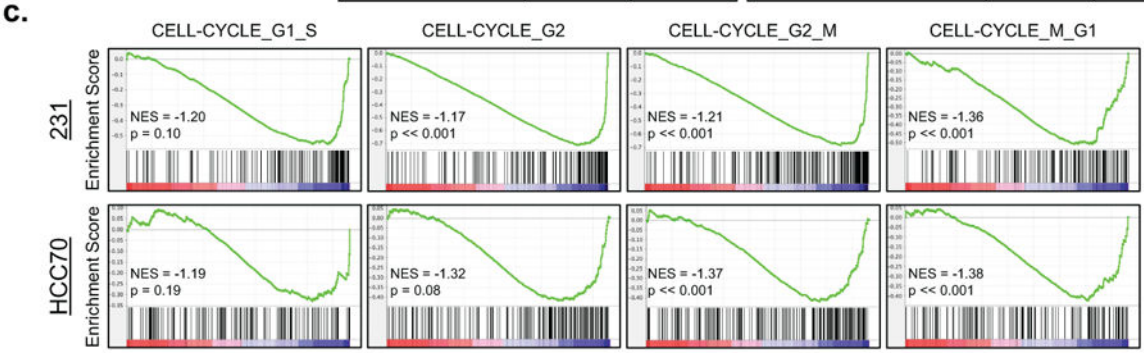

d.

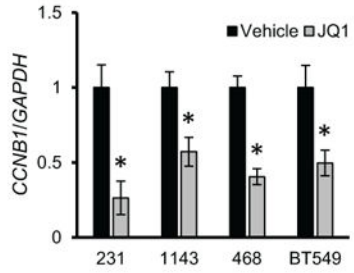

e.

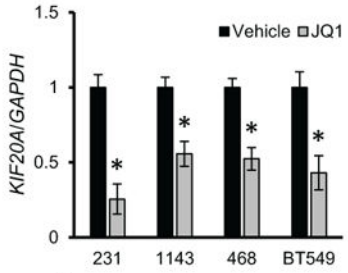

f.

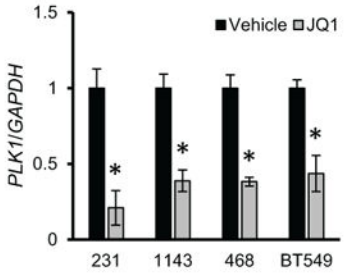

g.

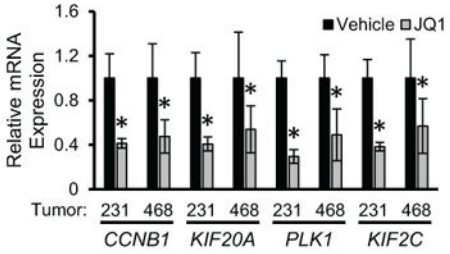

h.

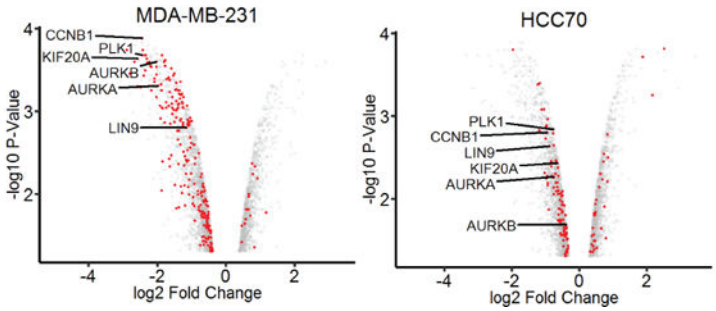

Figure 3. BET activity is necessary for sustained expression of cell cycle-associated genes

(**A–C**) MDA-MB-231 and HCC70 cells were treated for 72 hours with vehicle or 500 nM JQ1 and transcriptomes were analyzed using Affymetrix Human Gene 2.0 ST expression microarrays. (**A**) Venn diagram showing the number of genes whose expression significantly changed in each cell line as well as the number of genes commonly altered in both. (**B**) Top 5 non-overlapping Reactome terms for MDA-MB-231 (left) and HCC70 (right) cells. (**C**) GSEA of cell cycle-classifying genes whose expression was altered by JQ1 in MDA-MB-231 and HCC70 cells. (**D-F**) RT-qPCR analysis of three cell cycle/mitosis genes

Author Manuscript Author Manuscript Author Manuscript Author Manuscript

(*CCNB1*, *KIF20A*, and *PLK1*) in four TNBC cell lines treated with vehicle or 500 nM JQ1 for 24 hours. (**G**) RT-qPCR analysis of cell cycle and mitosis genes (*CCNB1*, *KIF20A*, *PLK1*, and *KIF2C*) in MDA-MB-231 (n=5) and MDA-MB-468 (n=10) tumors from orthotopically xenografted mice treated with vehicle or JQ1. (**H**) Volcano plots depicting mRNA log2 fold changes *versus* the corresponding $\log_{10}$ *p*-values for genes whose expression significantly changes in response to JQ1 in MDA-MB-231 (right) and HCC70 (left) cells after 72 hours. Red dots indicate genes that are critical for mitosis. For all bar graphs, data are presented as means ± SD (*=$p<0.05$ compared to vehicle).

Author Manuscript Author Manuscript Author Manuscript Author Manuscript

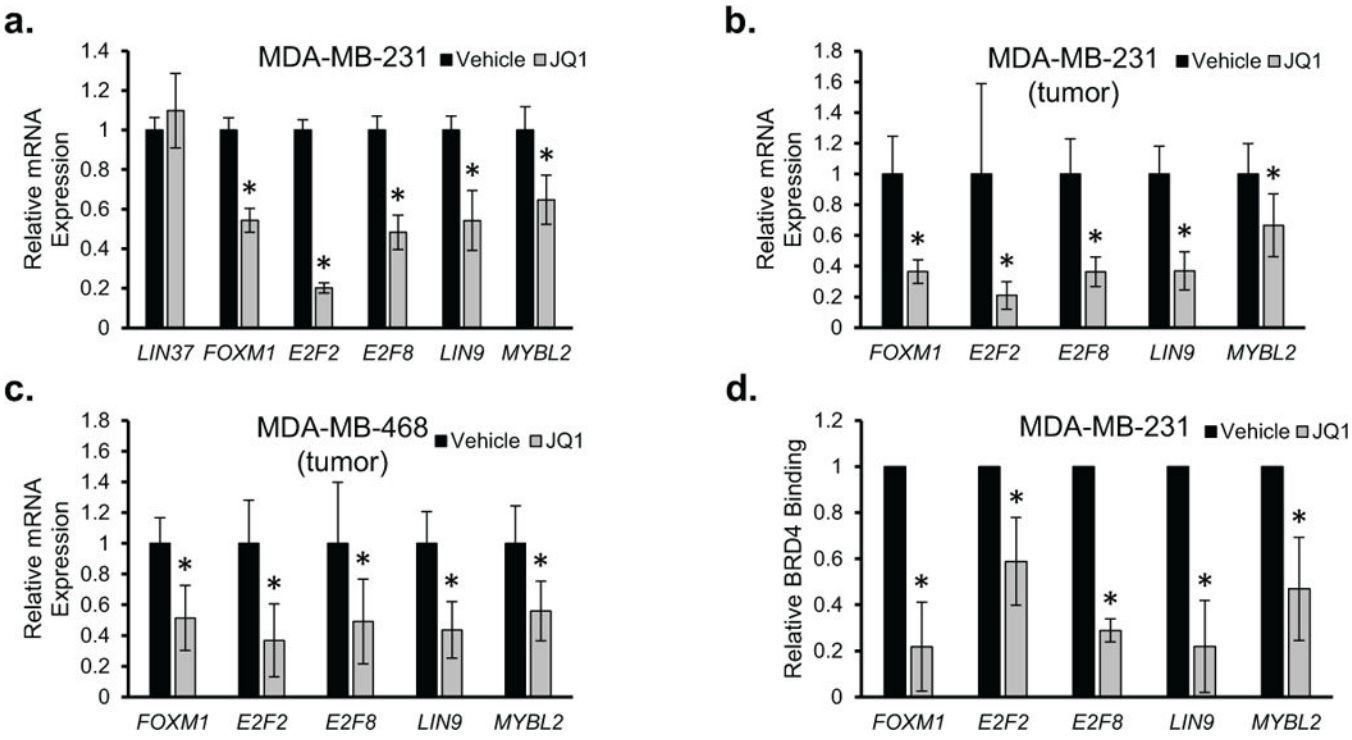

Figure 4. BET proteins directly modulate the mitotic transcriptional program

(**A**) RT-qPCR quantitation of the expression of selected mitosis-controlling transcription factors in MDA-MB-231 cells treated with vehicle or 500 nM JQ1 for 6 hours. (**B** and **C**) RT-qPCR analysis of BETi-repressed genes in tumors from vehicle- or JQ1-treated mice harboring (**B**) MDA-MB-231 (n=5) or (**C**) MDA-MB-468 (n=10) tumors. (**D**) Representative gene-specific ChIP-PCR analysis of MDA-MB-231 cells assessing binding of BRD4 to selected genes encoding mitosis-controlling transcription factors following treatment with vehicle or 500 nM JQ1 for 24 hours. For all graphs, data are presented as means ± SD (*=$p<0.05$ compared to vehicle or siNS).

Author Manuscript Author Manuscript Author Manuscript Author Manuscript

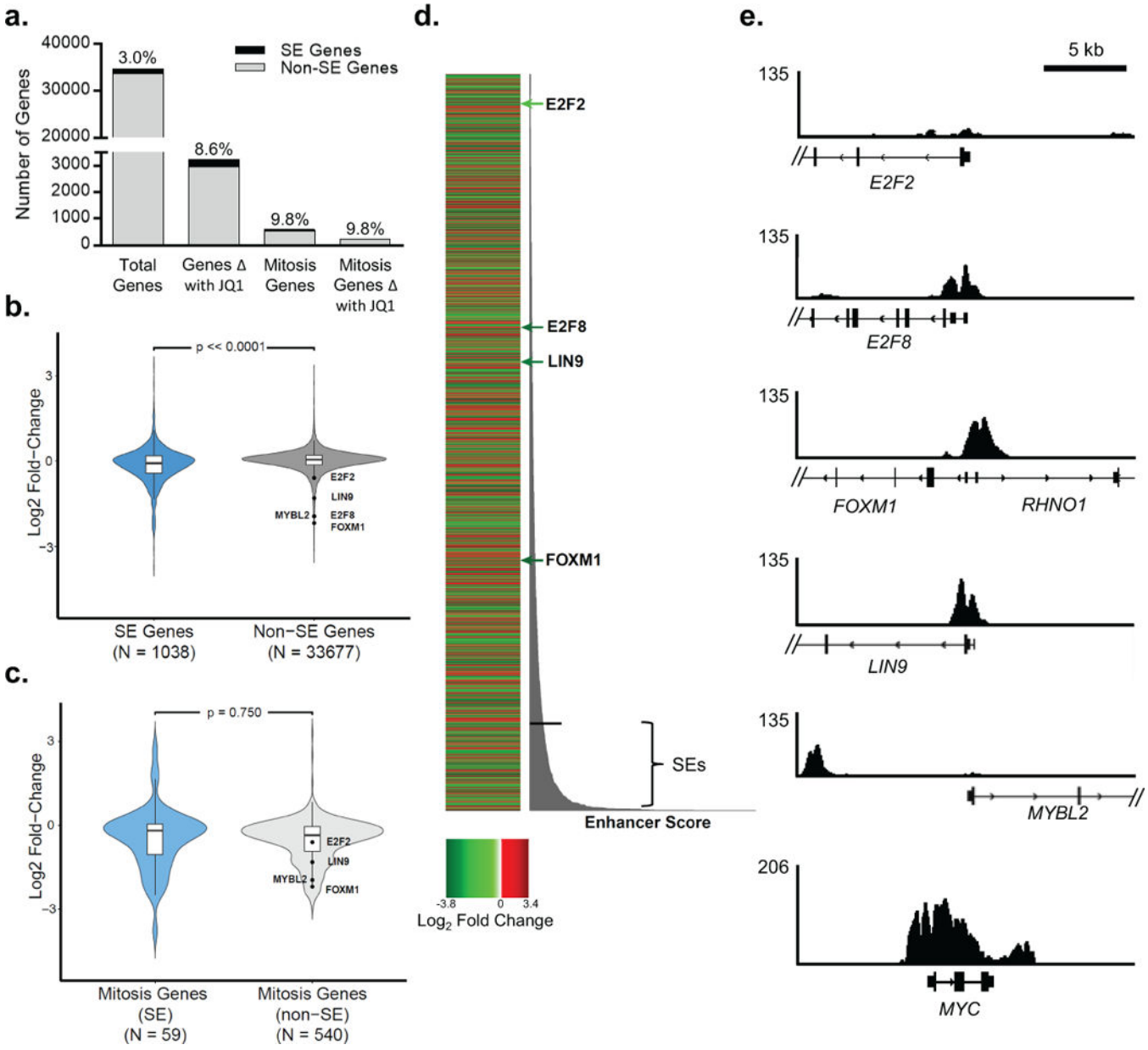

Figure 5. BETi suppress mitosis transcription factors in the absence of super-enhancers

Binding of H3K27Ac in MDA-MB-231 cells was analyzed using ChIP-seq. These data were compared with data generated from JQ1-treated MDA-MB-231 cells analyzed by gene expression microarray. (**A**) Number of genes in MDA-MB-231 cells that are associated with super-enhancers (SE genes) or lack super-enhancers (Non-SE genes). Total genes = all genes expressed in MDA-MB-231 cells based on microarray data. Mitosis genes = 599 genes identified by SuperPath as critical for mitosis. Percentages indicate the percent of genes that contain super-enhancers. (**B**) Violin plots depicting fold change in gene expression of SE-associated genes and non-SE-associated genes for all genes expressed in MDA-MB-231 cells ($p=4.2\times10^{-15}$). (**C**) Violin plots depicting fold change in gene expression of SE-associated genes and non-SE-associated genes for mitosis genes. (**D**) Heatmap showing log2

Author Manuscript Author Manuscript Author Manuscript Author Manuscript

fold change in expression of all JQ1-regulated genes in MDA-MB-231 cells ranked according to enhancer strength. The black line indicates the cut-off between SEs and typical enhancers. Four of the five BETi-regulated mitosis-regulating transcription factors are listed. *MYBL2* is absent because it lacks a specific enrichment of H3K27Ac binding within 10 kbp of its promoter. (**E**) ChIP-seq binding profiles for H3K27Ac at the promoter regions for five mitosis-regulating transcription factors. *MYC* is shown as a representative SE-associated gene.

Author Manuscript Author Manuscript Author Manuscript Author Manuscript

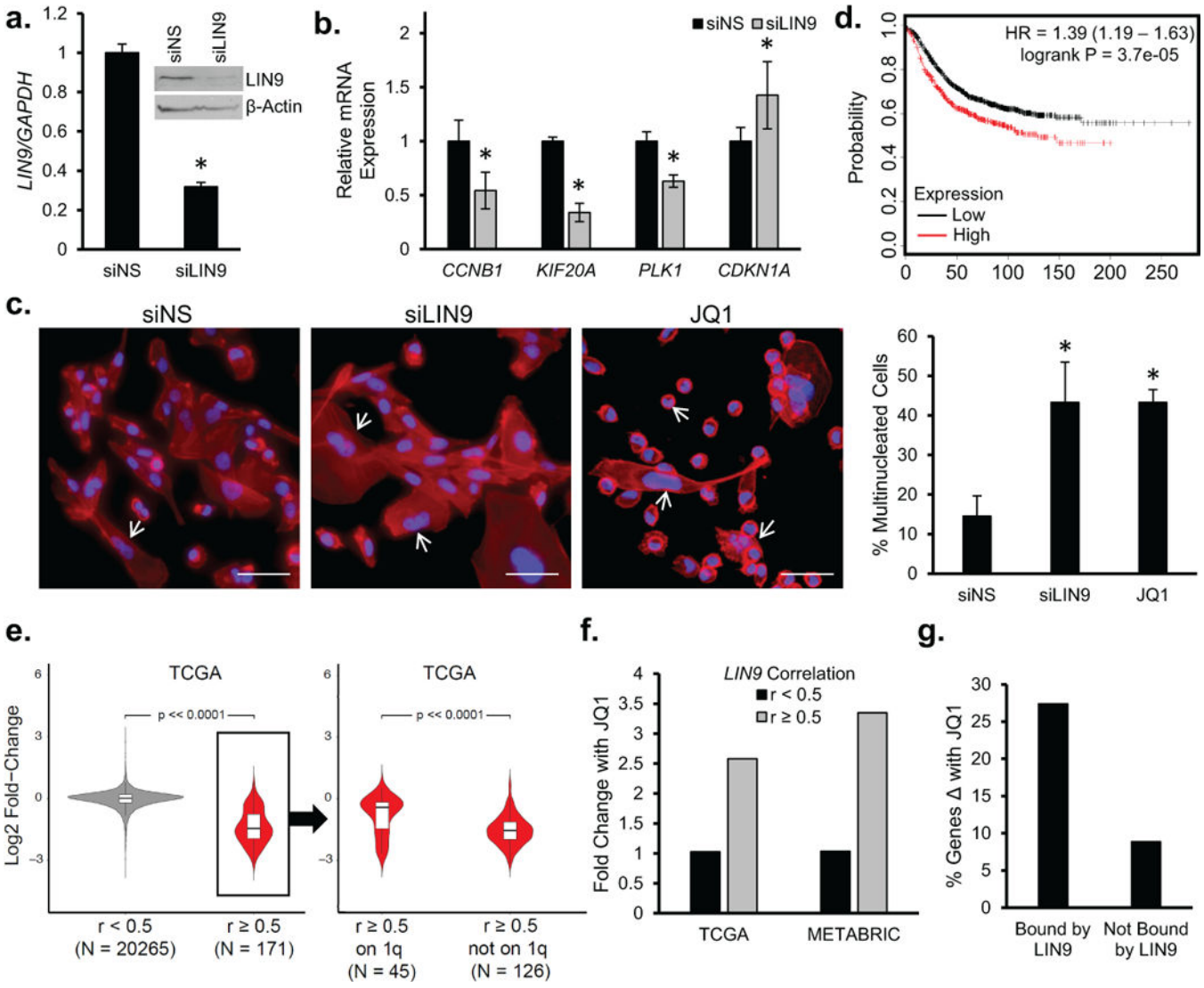

Figure 6. *LIN9* mediates the effects of BET inhibition

(**A**) Confirmation of siRNA-mediated knockdown of *LIN9* in MDA-MB-231 cells after five days. Inset is a representative western blot showing suppression of *LIN9* substantially reduces LIN9 protein. (**B**) RT-qPCR analysis of BETi-target genes in MDA-MB-231 cells following *LIN9* silencing. (**C**) Representative images (20×) of MDA-MB-231 cells following *LIN9* silencing that were stained with DAPI (blue, nuclei) and Texas Red-X phalloidin (red, actin cytoskeleton). MDA-MB-231 cells treated with 500 nM JQ1 are included as a comparison. Arrows indicate multinucleated cells. (**D**) Kaplan-Meier curve of relapse-free survival for breast cancer patients with high and low expression of *LIN9*. (**E**) Violin plots depicting BETi-induced expression (log2 fold change) of genes that are not correlated (r<0.5) or are correlated (r≥0.5) with *LIN9* expression. The right side of the panel depicts subdivision of genes that were correlated with *LIN9* (r≥0.5) according to residence on chromosome 1q *versus* their responsiveness to JQ1 (p-value for r<0.5 vs. r≥0.5 = 1.8×10^{-47}; p-value for r≥0.5 on 1q vs. not on 1q = 1.2×10^{-5}). r = Pearson's coefficient. (**F**) Absolute fold change in expression following JQ1 treatment of genes that are highly

Author Manuscript Author Manuscript Author Manuscript Author Manuscript

correlated with *LIN9* expression ($r \geq 0.5$) and those that are moderately or not correlated ($r < 0.5$) in the TCGA and METABRIC datasets. (**G**) Percent of genes changed with JQ1 that are bound by LIN9 or not bound by LIN9 ($p << 0.001$). For panels **A**, **B**, and **C**, data are presented as means ± SD (*=$p < 0.05$ compared to vehicle or siNS).